Journal of Engineering Mathematics (2023) 142:7
https://doi.org/10.1007/s10665-023-10295-2

Analytic solution and numerical validation of the transient regime in dry surface grinding

Juan Luis González-Santander[1]

Received: 24 May 2023 / Accepted: 29 August 2023

Abstract
In the framework of Samara–Valencia model for heat transfer in dry surface grinding, analytical expressions for the time-dependent temperature field of the workpiece during the transient regime in which the wheel is engaged (cut-in) and disengaged (cut-out) from the workpiece are calculated. The main assumption we consider is a constant heat flux profile along the contact zone between the wheel and the workpiece. According to the analytical expression obtained for the temperature field, a closed-form expression for the maximum temperature during the cut-in transient regime has been obtained. Further, a very rapid method for the numerical evaluation of maximum temperature during the cut-out is described. This maximum temperature is responsible of the thermal damage of the workpiece. Experimental evidence shows that the thermal damage risk is greater during the cut-out transient regime. The present analytical model reproduces this experimental feature. Finally, the analytical results have been numerically validated using FEM analysis and are intended to be very useful for the monitoring of the online grinding process in order to avoid thermal damage.

Keywords Dry surface grinding · Thermal damage · Transient regime

Mathematics Subject Classification 35K05 · 44A45 · 33C10 · 33B99

1 Introduction

Surface grinding is a machining process of metallic plates used for polishing a flat surface by using an abrasive wheel. The grinding wheel rotates at a high speed and slides over the workpiece surface, so that the surface material of the metallic plate being ground is removed. Most of the energy produced in grinding is converted into heat

✉ Juan Luis González-Santander
gonzalezmarjuan@uniovi.es

[1] Department of Mathematics, University of Oviedo, C/ Leopoldo Calvo Sotelo, 18, 33007 Oviedo, Asturias, Spain

Published online: 23 September 2023

due to friction between wheel and workpiece, and this heat is accumulated within the contact zone between both [1, 2]. The high temperatures reached during this machining process may produce an unacceptable decrease in the quality of workpieces, such as burning or residual stresses [3]. The author has presented and analytical approach in order to speed up the numerical evaluation of the maximum temperature in the stationary regime of dry surface grinding for and arbitrary heat flux profile entering into the workpiece [4]. However, the thermal damage risk is higher in the transient regime that occurs when the grinding wheel disengages from the workpiece (cut-out) [5]. A practical way to avoid the latter is to clamp the workpiece between plates in order to provide heat conduction at its ends. However, plates should be of the same width as the workpiece. Also, they have to be adjusted at the same level as the workpiece in order to control the depth of cut a (see Fig. 1). This disadvantage produces a significant delay in the online process. Therefore, an analytical expression would be very useful for the maximum temperature prediction in the transient regime with the workpiece alone.

The heat transfer in surface grinding is usually modelled by a flat strip heat source infinitely long along the z-axis and of δ width (m in SI units), sliding over the workpiece surface, and where the Cartesian coordinate system XYZ is fixed to the wheel (see Jaeger's model [6]). However, according to Fig. 1, the contact length between the grinding wheel and the workpiece is given by a circular arc, as it is considered for deep grinding in [7]. Nevertheless, in usual surface grinding conditions, the radius of the wheel is much greater than the depth of cut, $R \gg a$, thus we can model our heat source as a flat one, as aforementioned. The workpiece consists of a semi-infinite solid that is moving with respect to the wheel at a speed of $\vec{v}_{\mathrm{d}} = -v_{\mathrm{d}}\,\vec{i}$ (m s^{-1}). The temperature field in the workpiece $T\,(t, x, y)$ has to satisfy the convective heat equation [8, §1.7(2)]

$$\frac{\partial T}{\partial t} = \alpha\left(\frac{\partial^2 T}{\partial x^2} + \frac{\partial^2 T}{\partial y^2}\right) - v_{\mathrm{d}}\frac{\partial T}{\partial x}, \tag{1}$$

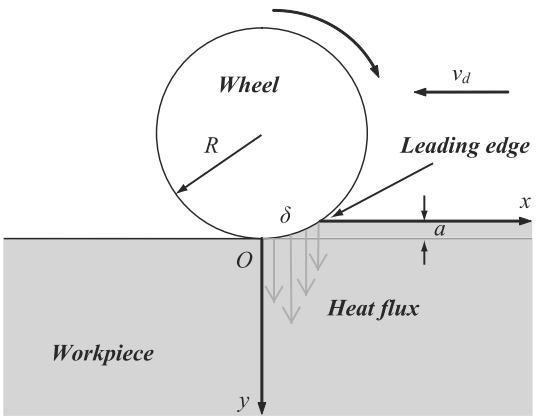

Fig. 1 Setup scheme in dry surface grinding

where α is the thermal diffusivity ($m^2\,s^{-1}$). Since initially the workpiece is at room temperature T_0 (K), (1) is subjected to the following initial condition:

$$T\,(0, x, y) = T_0. \tag{2}$$

According to the Samara–Valencia model [9], the boundary condition is given by

$$k\frac{\partial T}{\partial y}\,(t, x, 0) = b\,(t, x)\,[T\,(t, x, 0) - T_0] + d\,(t, x)\,, \tag{3}$$

where k ($W\,m^{-1}K^{-1}$) denotes the thermal conductivity, $b\,(t, x)$ is the heat transfer coefficient ($W\,m^{-2}\,K^{-1}$) between the workpiece and the environment (i.e. it considers the heat evacuated by convection due to liquid coolant applied onto the workpiece surface), and $d\,(t, x)$ takes into account the heat flux ($W\,m^{-2}$) entering into the workpiece due to friction between wheel and workpiece. It is worth noting that both $b\,(t, x)$ and $d\,(t, x)$ are input functions in the model and they have to be determined by other means such as experimental measurements and a partition model for the energy generated by friction in the contact zone [10].

According to the Samara–Valencia model [9], the solution of the boundary-value problem stated in (1)–(3) can be split in two terms

$$T\,(t, x, y) = T_0 + T^{(0)}\,(t, x, y) + T^{(1)}\,(t, x, y)\,, \tag{4}$$

where

$$T^{(0)}\,(t, x, y) = -\frac{1}{4\pi k}\int_0^t \frac{1}{s}\exp\left(\frac{-y^2}{4\alpha s}\right) \times \left\{\int_{-\infty}^{\infty} d\,(t - s, \xi)\exp\left(-\frac{(\xi - x - v_{\mathrm{d}}s)^2}{4\alpha s}\right)\mathrm{d}\xi\right\}\mathrm{d}s, \tag{5}$$

and

$$T^{(1)}\,(t, x, y) = \frac{1}{4\pi}\int_0^t \frac{1}{s}\exp\left(\frac{-y^2}{4\alpha s}\right)\left\{\int_{-\infty}^{\infty}\left(\frac{y}{2\alpha s} - \frac{b(t - s, \xi)}{k}\right) \times [T(t - s, \xi, 0) - T_0]\exp\left(-\frac{(\xi - x - v_{\mathrm{d}}s)^2}{4\alpha s}\right)\mathrm{d}\xi\right\}\mathrm{d}s. \tag{6}$$

Notice that $T^{(0)}\,(t, x, y)$ involves the part of the boundary condition (3) due to friction, and $T^{(1)}\,(t, x, y)$ the one due to convection. Notice as well that the time-dependent temperature field $T\,(t, x, y)$ given in (4) is an integral equation, since $T^{(1)}\,(t, x, y)$ involves the surface temperature rise $T\,(t, x, 0) - T_0$.

Wet grinding usually considers a constant heat transfer coefficient h on the surface, i.e. $b\,(t, x) = h$. However, in the case of dry grinding (adiabatic case), the convection

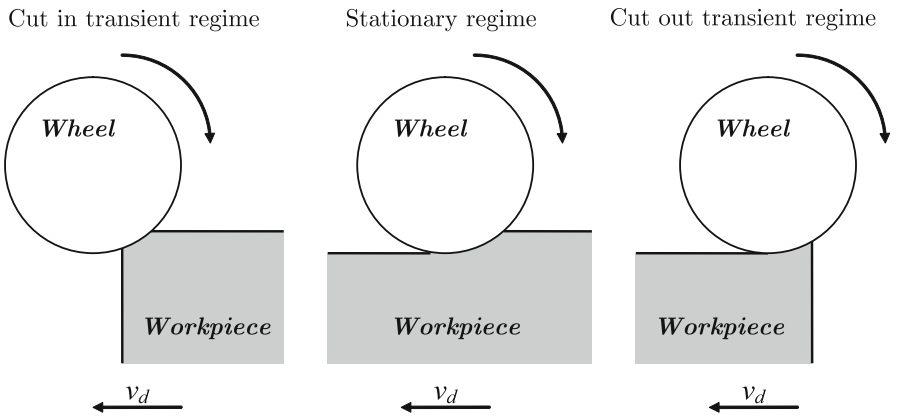

Fig. 2 Regimes in dry surface grinding

on the surface can be neglected, i.e. $b\,(t,x)=0$, and $T^{(0)}\,(t,x,y)=T^{(1)}\,(t,x,y)$ [11], thus (4) becomes

$$\begin{aligned} T\,(t,x,y) &= T_0 + 2\,T^{(0)}\,(t,x,y) \\ &= T_0 - \frac{1}{2\pi k}\int_0^t \frac{1}{s}\exp\left(\frac{-y^2}{4\alpha s}\right) \\ &\quad\times\left\{\int_{-\infty}^{\infty} d\,(t-s,\xi)\exp\left(-\frac{(\xi-x-v_{\mathrm{d}}s)^2}{4\alpha s}\right)\mathrm{d}\xi\right\}\mathrm{d}s. \end{aligned} \tag{7}$$

The above result is highly non-trivial and is termed as $T^{(0)}$*-theorem*.

Figure 2 shows three sequential regimes during grinding for the analysis of the temperature field: cut-in, stationary regime and cut-out. During the transient regime of the cut-in, the friction width increases linearly from zero to its stationary regime value. If the workpiece is long enough (this length depends on the thermal properties of the workpiece and the grinding conditions), then the temperature field reaches in practice the stationary regime (i.e. $\partial T/\partial t\approx 0$). The cut-out transient regime occurs during disengagement at the end of the grinding pass, decreasing the friction width from its value in the stationary regime to zero.

On the one hand, the workpiece temperature during the cut-in and cut- out transient regimes has been evaluated by using FEM analysis [5, 12]. On the other hand, an analytic model has been derived by the author in [13] considering a linear heat flux profile in dry surface grinding (i.e. $b\,(t,x)=0$). It is worth noting that an analytical solution is quite desirable because it needs much less computing resources than the FEM analysis. Also, from an analytical expression, the parametric dependence of the temperature field can be analysed directly. The goal of this paper is to extend the analytic model given in [13] considering a constant heat flux profile. From this solution, we propose a very rapid method to evaluate the maximum temperature during the transient regime (cut-in and cut-out).

This paper is organized as follows. Section 2 calculates the temperature field (7) for a continuous-acting constant heat flux profile in the stationary regime. From this result, an equation for maximum temperature computation is derived. An equation for the duration of the transient regime (relaxation time) and its approximation are also presented. Section 3 is devoted to the derivation of the temperature field during the transient regime of the cut-out. From this expression, an equation for the root searching of maximum temperature at the workpiece edge is derived. Section 4 redoes the calculations of Sect. 3 for the cut-in transient regime. In Sect. 5, some numerical simulations for the cut-in, cut-out and stationary regimes are presented, as well as the numerical validation using FEM analysis. The conclusions are summarized in Sect. 6.

2 Stationary regime

2.1 Temperature field

The heat source profile has been modelled as constant [14, 15], triangular [16, 17] or parabolic profile [18] along the friction zone between wheel and workpiece. As mentioned before, the transient regime during the cut-in and cut-out has been studied analytically considering a linear heat flux profile in [13]. In the present study, we consider a constant heat flux profile, hence we take the following $d\,(t, x)$ function in (7)

$$d\,(t, x) = -q\;\theta\,(x)\;\theta\,(\delta - x)\,, \tag{8}$$

where $\theta\,(x)$ denotes the Heaviside function [19, Eq. 1.16.13],

$$\theta\,(x) = \begin{cases} 1, & x > 0 \\ 0, & x \leq 0, \end{cases} \tag{9}$$

and q is the average heat flux ($\mathrm{W\,m^{-2}}$) over the grinding zone, $x \in [0, \delta]$. Defining the Peclet number Pe as (see [1, p. 160]):

$$\mathrm{Pe} = \frac{v_\mathrm{d}\,\delta}{4\alpha},$$

and considering the following dimensionless variables [20]:

$$\mathcal{T} = \frac{\pi k v_\mathrm{d}\,(T - T_0)}{2q\alpha}, \quad X = \frac{v_\mathrm{d}\,(x - \delta/2)}{2\alpha}, \quad Y = \frac{v_\mathrm{d} y}{2\alpha}, \quad \tau = \frac{v_\mathrm{d}\sqrt{t}}{2\sqrt{\alpha}}, \tag{10}$$

the time-dependent temperature field $\mathcal{T}\,(\tau, X, Y)$ for a constant heat flux profile in the dry case reads as [20]:

$$\mathcal{T}\,(\tau, X, Y) = \sqrt{\pi}\int_0^\tau \exp\left(-\frac{Y^2}{4w}\right)\mathrm{erf}\left(\frac{u}{2w} + w\right)\Big|_{u=X-\mathrm{Pe}}^{X+\mathrm{Pe}} \mathrm{d}w,$$

where the error function is defined as [21, Eq. 40:3:1]:

$$\operatorname{erf}(x) = \frac{2}{\sqrt{\pi}} \int_0^x \mathrm{e}^{-t^2}\, \mathrm{d}t. \tag{11}$$

Note that the time scaling in (10) is nonlinear, as in the case of the dimensionless parameter given in [8, Eq. 2.4(4)] for the heat transfer in a semi-infinite solid.

2.2 Maximum temperature

From a physical point of view, the maximum temperature $\mathcal{T}_{\max}$ must be reached in the stationary regime ($\tau \to \infty$), because the longer the heat source is acting, the greater is the temperature in the workpiece. Moreover, the location of the maximum temperature rise $X_{\max}$ must be on the surface ($Y = 0$), within the contact zone between wheel and workpiece, $X_{\max} \in [-\mathrm{Pe}, \mathrm{Pe}]$. For a mathematical approach to the latter, see [22]. Therefore, let us consider the surface temperature rise in the stationary regime with dimensionless variables $\mathcal{T}(X, 0)$. According to [23], we have the following expression for the dry case with a constant heat flux profile,

$$\mathcal{T}(X, 0) = \lim_{\tau \to \infty} \mathcal{T}(\tau, X, 0) = \mathrm{Jg}_0(u)\big|_{u=-X-\mathrm{Pe}}^{-X+\mathrm{Pe}}, \tag{12}$$

being (see [4] for the definition of this function),

$$\mathrm{Jg}_0(x) = \begin{cases} x\mathrm{e}^x \left\{K_0(|x|) + \operatorname{sgn}(x)\, K_1(|x|)\right\}, & x \neq 0, \\ 0, & x = 0, \end{cases} \tag{13}$$

where $K_\nu(z)$ denotes the Macdonald function of order ν. Since $\mathcal{T}(X, 0)$ is a differentiable function, a convenient way to evaluate the maximum temperature rise is to solve numerically all points X^* that satisfies

$$\frac{\partial \mathcal{T}(X^*, 0)}{\partial X} = 0, \qquad X^* \in [-\mathrm{Pe}, \mathrm{Pe}], \tag{14}$$

and then, the maximum is given by

$$\mathcal{T}_{\max} = \max_{X^*} \left[\mathcal{T}\left(X^*, 0\right)\right]. \tag{15}$$

In Sect. 5, we will check numerically that the root X^* is unique for a constant heat flux profile, so $X^* = X_{\max}$. According to [23], Eq. (14) is written as

$$\begin{aligned} &\mathrm{e}^{-\mathrm{Pe}} K_0(|X_{\max} + \mathrm{Pe}|) - \mathrm{e}^{\mathrm{Pe}} K_0(|X_{\max} - \mathrm{Pe}|) = 0, \\ &X_{\max} \in [-\mathrm{Pe}, \mathrm{Pe}]. \end{aligned} \tag{16}$$

Finally, according to (10), we have

$$T_{\max}^{\mathrm{Sta}} = T_0 + \frac{2q\alpha}{\pi k v_{\mathrm{d}}} \mathcal{T}\left(X_{\max}, 0\right) \tag{17}$$

2.3 Relaxation time

As aforementioned, the stationary regime is asymptotically reached at $t \to \infty$. In dimensionless variables, we have

$$\lim_{\tau \to \infty} \frac{\partial \mathcal{T}\left(\tau, X, Y\right)}{\partial \tau} = 0. \tag{18}$$

To avoid thermal damage, the location of the maximum temperature rise $X_{\max}$ is the most important one. Therefore, in order to estimate the duration of the transient regime (relaxation time), we can solve the following equation for $\tau^* > 0$:

$$\frac{\partial \mathcal{T}\left(\tau^*, X_{\max}, 0\right)}{\partial \tau} = \eta \approx 0. \tag{19}$$

According to [20], Eq. (19) is expressed in dimensionless variables as

$$\sqrt{\pi}\ \mathrm{erf}\left(\frac{u}{2\tau^*} + \tau^*\right)\Big|_{u=X_{\max}-\mathrm{Pe}}^{X_{\max}+\mathrm{Pe}} = \eta, \tag{20}$$

obtaining the following approximated expression for the relaxation time

$$\tau^* \approx \sqrt{\frac{1}{2}\mathrm{W}\left(8\left[\frac{\sinh \mathrm{Pe}}{\eta\, \mathrm{e}^{X_{\max}}}\right]^2\right)}, \tag{21}$$

where $W(z)$ denotes the Lambert-W function [24]. The approximation given in (21) can be used as starting iteration point for the numerical root searching of (20). Finally, according to (10), we have

$$t^* = \frac{4\alpha}{v_{\mathrm{d}}^2}\left(\tau^*\right)^2. \tag{22}$$

3 Transient regime in the cut-out

3.1 Temperature field

When the workpiece is disengaging from the grinding wheel, it occurs a transient regime because the workpiece can no longer be treated as infinite in the x direction (as in the stationary regime), and the friction area between wheel and workpiece is reduced from its initial width δ to 0. Figure 3 shows the relationship between the coordinate

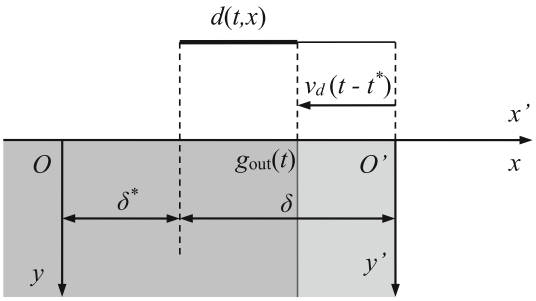

Fig. 3 Scheme of the transient regime during the cut-out

system fixed to the wheel XYZ and the one fixed to the workpiece $X'Y'Z'$, so

$$x = x' + \delta - v_{\mathrm{d}} \left(t - t^* \right), \tag{23}$$

where t^* is given by (22). Notice that initially (i.e. at $t = 0$), the system fixed to the wheel is separated from the final edge of the workpiece a distance $\delta^* + \delta$, being

$$\delta^* = v_{\mathrm{d}} t^*, \tag{24}$$

that is, the distance that the workpiece moves with respect to the wheel during the relaxation time t^*. Therefore, when the leading edge of the friction area reaches the workpiece edge, the temperature field has already arrived at the stationary regime.

Considering a constant heat flux profile as in (8), we have the following friction function for the cut-out transient regime,

$$d_{\mathrm{out}} \left(t, x \right) = -q \, \theta \left(x \right) \, \theta \left(g_{\mathrm{out}} \left(t \right) - x \right), \tag{25}$$

where

$$g_{\mathrm{out}} \left(t \right) = \begin{cases} \delta, & 0 \leq t < t^*, \\ \delta - v_{\mathrm{d}} \left(t - t^* \right), & t^* \leq t < t^* + t_{\mathrm{p}}, \\ 0, & t \geq t^* + t_{\mathrm{p}}, \end{cases} \tag{26}$$

and t_{p} is the time that the workpiece needs to move a distance δ (i.e. the duration of the transient regime, both in the cut-in and in the cut-out):

$$t_{\mathrm{p}} = \frac{\delta}{v_{\mathrm{d}}}. \tag{27}$$

Applying the results of the Appendix (A9) and (A11), an abbreviated form for the $g_{\mathrm{out}} \left(t \right)$ function is

$$g_{\mathrm{out}} \left(t \right) = \min \left(\max \left(\delta - v_{\mathrm{d}} \left(t - t^* \right), 0 \right), \delta \right), \tag{28}$$

where notice that

$$g_{\mathrm{out}} \left(0 \right) = \delta. \tag{29}$$

Substituting the friction function (25) into (7), and taking into account the definition of the error function (11), after some algebra, we arrive at

$$T^{\text{out}}(t,x,y) = T_0 + \frac{q\sqrt{\alpha}}{2\sqrt{\pi}k}\int_0^t \frac{1}{\sqrt{s}}\exp\left(\frac{-y^2}{4\alpha s}\right)\text{erf}\left(\frac{u-x-v_{\text{d}}s}{2\sqrt{\alpha s}}\right)\Bigg|_{u=0}^{g_{\text{out}}(t-s)} \text{d}s. \quad (30)$$

Notice that (30) provides the temperature field for a semi-infinite solid in the coordinate system fixed to the wheel XYZ. Performing the change of coordinates (23), we have the temperature field related to the workpiece

$$T_w^{\text{out}}\left(t,x',y\right) = T^{\text{out}}\left(t,x'+\delta-v_{\text{d}}\left(t-t^*\right),y\right). \quad (31)$$

Now, applying the method of images [25, Sect. 8.5.8], the temperature rise field with respect to the initial temperature T_0 for a half semi-infinite solid (i.e. the workpiece shown in Fig. 3) is

$$\begin{aligned} T_{w/2}^{\text{out}}\left(t,x',y\right) - T_0 &= \left[T_w^{\text{out}}\left(t,x',y\right) - T_0\right] + \left[T_w^{\text{out}}\left(t,-x',y\right) - T_0\right] \\ &= T^{\text{out}}\left(t,x'+\delta-v_{\text{d}}\left(t-t^*\right),y\right) - T_0 \\ &\quad + T^{\text{out}}\left(t,-x'+\delta-v_{\text{d}}\left(t-t^*\right),y\right) - T_0. \end{aligned} \quad (32)$$

Note that $T_{w/2}^{\text{out}}\left(t,x',y\right)$ satisfies the boundary condition

$$\frac{\partial T_{w/2}^{\text{out}}(t,0,y)}{\partial x'} = 0, \quad (33)$$

that is, there is not convection at the workpiece boundary $x' = 0$, as it should be in the case of dry grinding.

3.2 Maximum temperature at the edge

According to [5], the risk of thermal damage during the transient regime of the cut-out is higher than in the stationary regime, because the workpiece material is suddenly unavailable to dissipate heat. This suggest that the maximum temperature should be located at the end of the workpiece (i.e. $x' = 0$). Furthermore, similarly to the stationary regime, the maximum must be reached on the surface ($y = 0$) within the friction area between wheel and workpiece. Therefore, since the transient regime of the cut-out occurs within the time interval $t \in \left(t^*, t^* + t_{\text{p}}\right)$ (see Fig. 3) let us consider the temperature evolution at the edge of the workpiece, that is, according to (30) and (32), the following function:

$$T_{w/2}^{\text{out}}(t,0,0) = T_0 + 2\,T^{\text{out}}\left(t,\delta-v_{\text{d}}\left(t-t^*\right),0\right)$$

$$= T_0 + \frac{q\sqrt{\alpha}}{\sqrt{\pi}k}\int_0^t \operatorname{erf}\left(\frac{u-\delta+v_\mathrm{d}\left(t-t^*-s\right)}{2\sqrt{\alpha s}}\right)\Bigg|_{u=0}^{g_\mathrm{out}(t-s)}\frac{\mathrm{d}s}{\sqrt{s}}. \tag{34}$$

In order to find the maximum temperature $T_\mathrm{max}^\mathrm{out}$ that the workpiece edge reaches, let us solve the equation:

$$\frac{\partial T_{w/2}^\mathrm{out}\left(t_\mathrm{max},0,0\right)}{\partial t} = 0, \quad t_\mathrm{max}\in\left(t^*, t^*+t_\mathrm{p}\right), \tag{35}$$

so

$$T_\mathrm{max}^\mathrm{out} = T_{w/2}^\mathrm{out}\left(t_\mathrm{max},0,0\right). \tag{36}$$

By using the Leibniz's theorem for differentiation of integrals [19, Eq. 1.5.22]

$$\frac{\mathrm{d}}{\mathrm{d}t}\int_{\phi_1(t)}^{\phi_2(t)} f\left(s,t\right)\mathrm{d}s = f\left(\phi_2\left(t\right),t\right)\frac{\mathrm{d}\phi_2}{\mathrm{d}t} - f\left(\phi_1\left(t\right),t\right)\frac{\mathrm{d}\phi_1}{\mathrm{d}t} + \int_{\phi_1(t)}^{\phi_2(t)}\frac{\partial f\left(s,t\right)}{\partial t}\mathrm{d}s. \tag{37}$$

and applying (29), as well as the property given in the Appendix (A13), so that

$$\frac{\mathrm{d}}{\mathrm{d}t}g_\mathrm{out}\left(t-s\right) = -v_\mathrm{d}\,\theta\left(\delta - v_\mathrm{d}\left(t-t^*-s\right)\right)\theta\left(v_\mathrm{d}\left(t-t^*-s\right)\right), \tag{38}$$

after some algebra, we have

$$\begin{aligned}\frac{\partial T_{w/2}^\mathrm{out}\left(t,0,0\right)}{\partial t} = {}& \frac{1}{\sqrt{t}}\operatorname{erf}\left(\frac{u+v_\mathrm{d}t^*}{2\sqrt{\alpha t}}\right)\Bigg|_{u=0}^{\delta} \\ &+\frac{v_\mathrm{d}}{\sqrt{\pi\alpha}}\int_0^t\frac{\mathrm{d}s}{s}\left\{\exp\left(-\left[\frac{g_\mathrm{out}\left(t-s\right)-\delta+v_\mathrm{d}\left(t-t^*-s\right)}{2\sqrt{\alpha s}}\right]^2\right)\right. \\ &\left[1-\theta\left(\delta-v_\mathrm{d}\left(t-t^*-s\right)\right)\theta\left(v_\mathrm{d}\left(t-t^*-s\right)\right)\right] \\ &\left.-\exp\left(-\left[\frac{-\delta+v_\mathrm{d}\left(t-t^*-s\right)}{2\sqrt{\alpha s}}\right]^2\right)\right\}.\end{aligned} \tag{39}$$

Apply now the result given in the Appendix, i.e. (A14), to obtain

$$\frac{\partial T^{\text{out}}_{w/2}(t,0,0)}{\partial t} = \frac{1}{\sqrt{t}}\,\text{erf}\left(\frac{u+v_{\text{d}}t^*}{2\sqrt{\alpha t}}\right)\Bigg|_{u=0}^{\delta} + \frac{v_{\text{d}}}{\sqrt{\pi\alpha}}\int_0^t \frac{\text{d}s}{s}\left\{\exp\left(-\left[\frac{g_{\text{out}}(t-s)-\delta+v_{\text{d}}(t-t^*-s)}{2\sqrt{\alpha s}}\right]^2\right)\left[\theta\left(-v_{\text{d}}\left(t-t^*-s\right)\right)+\theta\left(v_{\text{d}}\left(t-t^*-s\right)-\delta\right)\right] - \exp\left(-\left[\frac{-\delta+v_{\text{d}}(t-t^*-s)}{2\sqrt{\alpha s}}\right]^2\right)\right\}. \tag{40}$$

Recall the definition of the $g_{\text{out}}(t)$ given in (28) and apply the result given in the Appendix, i.e. (A17), hence

$$\begin{aligned} &g_{\text{out}}(t-s)-\delta+v_{\text{d}}\left(t-t^*-s\right)\\ &=\min\left(\max\left(\delta-v_{\text{d}}\left(t-t^*-s\right),0\right)\right)-\left(\delta-v_{\text{d}}\left(t-t^*-s\right)\right)\\ &=-\left(\delta-v_{\text{d}}\left(t-t^*-s\right)\right)\theta\left(v_{\text{d}}\left(t-t^*-s\right)-\delta\right)\\ &\quad+v_{\text{d}}\left(t-t^*-s\right)\theta\left(-v_{\text{d}}\left(t-t^*-s\right)\right). \end{aligned}$$

However,

$$\theta\left(v_{\text{d}}\left(t_{\max}-t^*-s\right)-\delta\right)=0, \tag{41}$$

since the condition $\delta < v_{\text{d}}\left(t_{\max}-t^*-s\right)$ is never satisfied because the integration variable is positive $s>0$ and, according to (27) and (35), $t^* < t_{\max} < t^*+\delta/v_{\text{d}}$.

Therefore, (35) is reduced to

$$\begin{aligned} 0 = &\frac{1}{\sqrt{t_{\max}}}\,\text{erf}\left(\frac{u+v_{\text{d}}t^*}{2\sqrt{\alpha\, t_{\max}}}\right)\Bigg|_{u=0}^{\delta}\\ &-\frac{v_{\text{d}}}{\sqrt{\pi\alpha}}\int_0^{t_{\max}}\frac{\text{d}s}{s}\left[\exp\left(-\left[\frac{\delta-v_{\text{d}}(t_{\max}-t^*-s)}{2\sqrt{\alpha s}}\right]^2\right)\right.\\ &\left.-\exp\left(-\left[\frac{v_{\text{d}}(t_{\max}-t^*-s)}{2\sqrt{\alpha s}}\right]^2\right)\theta\left(-v_{\text{d}}\left(t_{\max}-t^*-s\right)\right)\right],\\ &t_{\max}\in\left(t^*,t^*+t_{\text{p}}\right). \end{aligned} \tag{42}$$

4 Transient regime in the cut-in

4.1 Temperature field

During the transient regime associated with the initial engagement of the grinding wheel to the workpiece, the friction zone increases from width 0 to δ. Figure 4 presents the relationship between both coordinate systems, one fixed to the wheel XYZ and the other fixed to the workpiece $X'Y'Z'$. Notice that initially (i.e. at $t=0$) the system fixed to the wheel is separated a distance δ from the final edge of the workpiece.

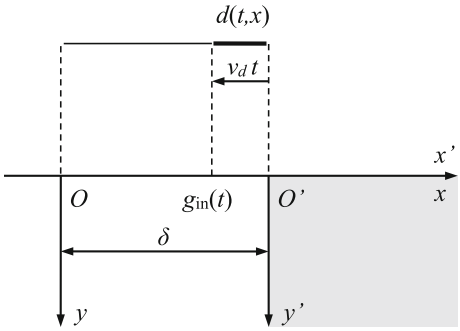

Fig. 4 Scheme of the transient regime during the cut-in

Considering a constant heat flux profile as in (8), we have the following friction function for the cut-in transient regime:

$$d_{\text{in}}\left(t,x\right)=-q\;\theta\left(x-g_{\text{in}}\left(t\right)\right)\;\theta\left(\delta-x\right),\tag{43}$$

where

$$g_{\text{in}}\left(t\right)=\begin{cases}\delta-v_{\text{d}}t, & 0\leq t<t_{\text{p}},\\ 0, & t\geq t_{\text{p}}.\end{cases}\tag{44}$$

According to the definition of the max function given in the Appendix (A1), since $t\geq 0$, an abbreviated form for the $g_{\text{in}}\left(t\right)$ function is

$$g_{\text{in}}\left(t\right)=\max\left(\delta-v_{\text{d}}t,0\right),\tag{45}$$

where notice that

$$g_{\text{in}}\left(0\right)=\delta.\tag{46}$$

Substituting the friction function (43) into (7) and taking into account (11), we arrive at

$$T^{\text{in}}\left(t,x,y\right)=T_0+\frac{q\sqrt{\alpha}}{2\sqrt{\pi}k}\int_0^t\exp\left(\frac{-y^2}{4\alpha s}\right)\operatorname{erf}\left(\frac{u-x-v_{\text{d}}s}{2\sqrt{\alpha s}}\right)\Bigg|_{u=g_{\text{in}}(t-s)}^{\delta}\frac{\text{d}s}{\sqrt{s}}.\tag{47}$$

Similarly to (32), the temperature rise field of a half semi-infinite solid in the coordinate system fixed to the workpiece is

$$\begin{aligned}T_{w/2}^{\text{in}}\left(t,x',y\right)-T_0=&\,T^{\text{in}}\left(t,x'+\delta-v_{\text{d}}t,y\right)-T_0\\&+T^{\text{in}}\left(t,-x'+\delta-v_{\text{d}}t,y\right)-T_0.\end{aligned}\tag{48}$$

4.2 Maximum temperature at the edge

Similarly to the cut-out case, let us consider the temperature evolution at the edge of the workpiece, that is to say, according to (47) and (48), the following function:

$$\begin{aligned} T^{\text{in}}_{w/2}(t,0,0) &= T_0 + 2\,T^{\text{in}}(t,\delta - v_{\text{d}}t,0) \\ &= T_0 + \frac{q\sqrt{\alpha}}{\sqrt{\pi}k}\int_0^t \text{erf}\left(\frac{u-\delta+v_{\text{d}}(t-s)}{2\sqrt{\alpha s}}\right)\Bigg|_{u=g_{\text{in}}(t-s)}^{\delta}\frac{\text{d}s}{\sqrt{s}}. \end{aligned} \tag{49}$$

In order to find the maximum temperature $T^{\text{in}}_{\text{max}}$ that the workpiece edge reaches, let us solve the equation

$$\frac{\partial T^{\text{in}}_{w/2}(t_{\text{max}},0,0)}{\partial t} = 0, \tag{50}$$

so

$$T^{\text{in}}_{\text{max}} = T^{\text{in}}_{w/2}(t_{\text{max}},0,0)\,. \tag{51}$$

By using again Leibniz's theorem for differentiation of integrals (37), and applying the result given in the Appendix, i.e. (A7), so that

$$\frac{\text{d}}{\text{d}t}g_{\text{in}}(t-s) = \frac{\text{d}}{\text{d}t}\max\left(\delta - v_{\text{d}}(t-s),0\right) = -v_{\text{d}}\,\theta\left(\delta - v_{\text{d}}(t-s)\right), \tag{52}$$

we arrive at

$$\begin{aligned} &\frac{\partial T^{\text{in}}_{w/2}(t,0,0)}{\partial t} \\ &= \frac{v_{\text{d}}}{\sqrt{\pi\alpha}}\int_0^t \frac{\text{d}s}{s}\left\{\exp\left(-\left[\frac{v_{\text{d}}(t-s)}{2\sqrt{\alpha\,s}}\right]^2\right)\right. \\ &\quad \left. + \exp\left(-\left[\frac{g_{\text{in}}(t-s)-\delta+v_{\text{d}}(t-s)}{2\sqrt{\alpha\,s}}\right]^2\right)\left[\theta\left(\delta - v_{\text{d}}(t-s)\right)-1\right]\right\}. \end{aligned}$$

Applying (A15), i.e.

$$\begin{aligned} \theta\left(\delta - v_{\text{d}}(t-s)\right) - 1 &= \theta\left(v_{\text{d}}(t-s)-\delta\right) \\ &= \theta\left(v_{\text{d}}\left(t-t_{\text{p}}-s\right)\right), \end{aligned}$$

and the result given in the Appendix (A5), i.e.

$$\begin{aligned} g_{\text{in}}(t-s) - \delta + v_{\text{d}}(t-s) &= \max\left(\delta - v_{\text{d}}(t-s),0\right) - \left[\delta - v_{\text{d}}(t-s)\right] \\ &= \max\left(v_{\text{d}}(t-s)-\delta,0\right) \\ &= \max\left(v_{\text{d}}\left(t-t_{\text{p}}-s\right),0\right) \end{aligned}$$

we arrive at

$$\begin{aligned}&\frac{\partial T_{w/2}^{\mathrm{in}}\left(t,0,0\right)}{\partial t}\\&=\frac{v_{\mathrm{d}}}{\sqrt{\pi\alpha}}\int_0^t\frac{\mathrm{d}s}{s}\left\{\exp\left(-\left[\frac{v_{\mathrm{d}}\left(t-s\right)}{2\sqrt{\alpha\, s}}\right]^2\right)\right.\\&\left.-\exp\left(-\left[\frac{\max\left(v_{\mathrm{d}}\left(t-t_{\mathrm{p}}-s\right),0\right)}{2\sqrt{\alpha\, s}}\right]^2\right)\theta\left(v_{\mathrm{d}}\left(t-t_{\mathrm{p}}-s\right)\right)\right\}.\end{aligned}\tag{53}$$

Theorem 1 *The maximum temperature in the cut-in is reached at*

$$t_{\max}=t_{\mathrm{p}}=\frac{\delta}{v_{\mathrm{d}}},\tag{54}$$

thus

$$T_{\max}^{\mathrm{in}}=T_{w/2}^{\mathrm{in}}\left(t_{\mathrm{p}},0,0\right).\tag{55}$$

Proof On the one hand, for $t<t_{\mathrm{p}}$, we have that $v_{\mathrm{d}}\left(t-t_{\mathrm{p}}-s\right)-\delta<0$, since the integration variable is positive, $s>0$. Therefore, $\theta\left(v_{\mathrm{d}}\left(t-t_{\mathrm{p}}-s\right)\right)=0$ and (53) reduces to

$$\left.\frac{\partial T_{w/2}^{\mathrm{in}}\left(t,0,0\right)}{\partial t}\right|_{t<t_{\mathrm{p}}}=\frac{v_{\mathrm{d}}}{\sqrt{\pi\alpha}}\int_0^t\exp\left(-\left[\frac{v_{\mathrm{d}}\left(t-s\right)}{2\sqrt{\alpha\, s}}\right]^2\right)\frac{\mathrm{d}s}{s}>0.\tag{56}$$

Consequently, $T_{w/2}^{\mathrm{in}}\left(t,0,0\right)$ is an increasing function for $t<t_{\mathrm{p}}$, thus the maximum temperature is not found for $t<t_{\mathrm{p}}$.

On the other hand, for $t>t_{\mathrm{p}}$, we have that

$$\theta\left(v_{\mathrm{d}}\left(t-t_{\mathrm{p}}-s\right)\right)=\begin{cases}1,\ s<t-t_{\mathrm{p}},\\0,\ s>t-t_{\mathrm{p}},\end{cases}\tag{57}$$

thus

$$\begin{aligned}F\left(t\right):=\frac{\sqrt{\pi\alpha}}{v_{\mathrm{d}}}\left.\frac{\partial T_{w/2}^{\mathrm{in}}\left(t,0,0\right)}{\partial t}\right|_{t>t_{\mathrm{p}}}&=\int_0^t\exp\left(-\left[\frac{v_{\mathrm{d}}\left(t-s\right)}{2\sqrt{\alpha\, s}}\right]^2\right)\frac{\mathrm{d}s}{s}\\&-\int_0^{t-t_{\mathrm{p}}}\exp\left(-\left[\frac{v_{\mathrm{d}}\left(t-t_{\mathrm{p}}-s\right)}{2\sqrt{\alpha\, s}}\right]^2\right)\frac{\mathrm{d}s}{s}.\end{aligned}\tag{58}$$

Perform now the changes of variables $\sigma=v_{\mathrm{d}}^2\, s/\left(4\alpha\right)$, $\xi=v_{\mathrm{d}}^2\, t/\left(4\alpha\right)$, and $\xi_{\mathrm{p}}=v_{\mathrm{d}}^2\, t_{\mathrm{p}}/\left(4\alpha\right)$, to obtain

$$F\left(\xi\right)=u\left(\xi\right)-u\left(\xi-\xi_{\mathrm{p}}\right),\tag{59}$$

where we have defined

$$u(\xi) = \mathrm{e}^{2\xi} \int_0^{\xi} \exp\left(-\frac{\xi^2}{\sigma} - \sigma\right) \frac{\mathrm{d}\sigma}{\sigma}. \tag{60}$$

Notice that performing the change of variables $w = \xi^2/\sigma$ we have that

$$\int_0^{\xi} \exp\left(-\frac{\xi^2}{\sigma} - \sigma\right) \frac{\mathrm{d}\sigma}{\sigma} = \int_{\xi}^{\infty} \exp\left(-\frac{\xi^2}{w} - w\right) \frac{\mathrm{d}w}{w}, \tag{61}$$

so that, applying the property (61) and the integral representation of $K_0(z)$ [19, Eq. 10.32.10], we have

$$\begin{aligned} K_0(2\xi) &= \frac{1}{2} \int_0^{\infty} \exp\left(-\frac{\xi^2}{\sigma} - \sigma\right) \frac{\mathrm{d}\sigma}{\sigma} \\ &= \frac{1}{2} \left\{ \int_0^{\xi} \exp\left(-\frac{\xi^2}{\sigma} - \sigma\right) \frac{\mathrm{d}\sigma}{\sigma} + \int_{\xi}^{\infty} \exp\left(-\frac{\xi^2}{\sigma} - \sigma\right) \frac{\mathrm{d}\sigma}{\sigma} \right\} \\ &= \int_0^{\xi} \exp\left(-\frac{\xi^2}{\sigma} - \sigma\right) \frac{\mathrm{d}\sigma}{\sigma}. \end{aligned}$$

Therefore

$$u(\xi) = \mathrm{e}^{2\xi} K_0(2\xi). \tag{62}$$

Note that

$$u'(\xi) = 2\,\mathrm{e}^{2\xi} [K_0(2\xi) - K_1(2\xi)] < 0, \tag{63}$$

because $K_0(x) < K_1(x)$ due to the integral representation [19, Eq. 10.32.9]

$$K_\nu(z) = \int_0^{\infty} \exp(-z\cosh t)\cosh(\nu t)\,\mathrm{d}t. \tag{64}$$

Since $u(\xi)$ is a decreasing function, according to (59), we have $F(\xi) < 0$. Therefore, according to (58), $T^{\mathrm{in}}_{w/2}(t, 0, 0)$ is a decreasing function for $t > t_{\mathrm{p}}$, i.e.

$$\left.\frac{\partial T^{\mathrm{in}}_{w/2}(t, 0, 0)}{\partial t}\right|_{t > t_{\mathrm{p}}} < 0. \tag{65}$$

From (56) and (65), we conclude that the maximum temperature is reached at $t_{\max} = t_{\mathrm{p}}$, as we wanted to prove. □

5 Numerical results

5.1 Analytic simulation

Table 1 shows three sets of parameters (in SI units) for the numerical simulations.

Table 1 Simulation parameters in SI units and dimensionless Peclet number

	Material	Data 1 Titanium	Data 2 Steel	Data 3 Sapphire
Workpiece	k	13	60.5	46
	α	4.23×10^{-6}	1.77×10^{-5}	1.51×10^{-5}
	δ	2.66×10^{-3}	1.4×10^{-3}	2.5×10^{-3}
Grinding	q	5.89×10^{7}	1.4×10^{7}	1.8×10^{7}
Regime	v_{d}	0.53	3.3×10^{-2}	3.3×10^{-2}
	T_0	300	300	300
Peclet num.	Pe	83.4	0.65	1.36

Table 2 Characteristic times in the transient regime

	Data 1	Data 2	Data 3
t^* (approx.) [s]	1.02×10^{-2}	0.435	0.452
t^* (exact) [s]	6.52×10^{-3}	0.434	0.448
t_{p} [s]	5.02×10^{-3}	4.24×10^{-2}	7.58×10^{-2}

Data set 1 considers a titanium alloy VT20 workpiece, whose thermal properties are given in [26]. The grinding regime for this simulation can be found in [9]. Data set 2 considers carbon steel and data set 3 aluminium oxide Al_2O_3 (sapphire) as workpiece materials, both in creep feed grinding regime [27], i.e. "low speed condition" since $\mathrm{Pe} \approx 1$ (see [1, pp. 159–160]).

Table 2 presents the characteristic times for the three data sets. We have used (21) and (22) to compute an approximated value of t^*. It is worth noting that the relaxation time approximation yields very accurate results for data sets 2 and 3. The approximation given in (21) for τ^* has been used as starting iteration point of Newton's method in the root searching of (20), where we have taken $\eta = 10^{-3}$ for all data sets. According to (10) and the order of magnitude of the parameters given in Tables 1 and 2, a value of $\eta = 10^{-3}$ indicates that $\partial T/\partial t \approx 1\ \mathrm{K\,s^{-1}}$, i.e. a practically null slope (see Figs. 7 and 6), which is consistent with (19). Also, notice that t^* is much larger in creep feeding (data sets 2 and 3) than in the case of data set 1.

Figure 5 shows the surface temperature in the stationary regime for the three data sets. Note that for data set 1 (titanium) there is not temperature rise in front of the leading edge because of the high speed of the grinding feed, just the opposite to data sets 2 (steel) and 3 (sapphire), where we have creep feeding.

Figure 6 shows the absolute temperature at the workpiece edge for the three data sets during the cut-out transient regime, $T^{\mathrm{out}}_{w/2}(t, 0, 0)$. Note that now the graphs do not begin at room temperature T_0 because when the grinding wheel reaches the end of the workpiece, the temperature field is almost in the stationary regime, $t > t^*$. Notice as well that the maximum temperature falls within the interval $\left(t^*, t^* + t_{\mathrm{p}}\right)$, according to (35).

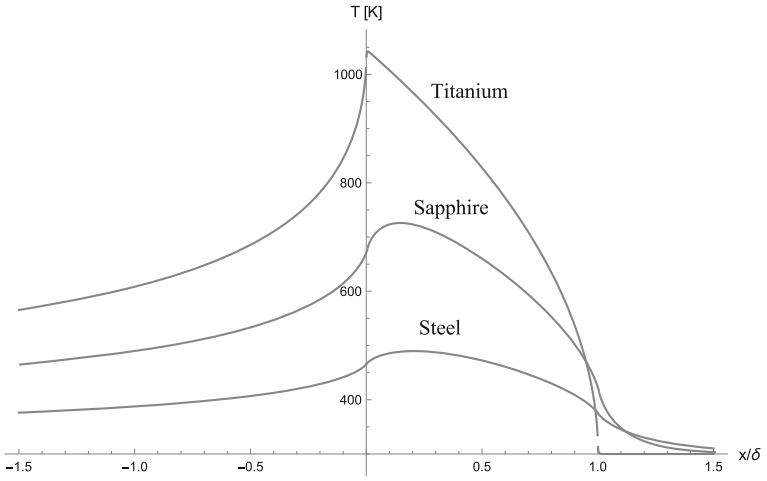

Fig. 5 Surface temperature in the stationary regime

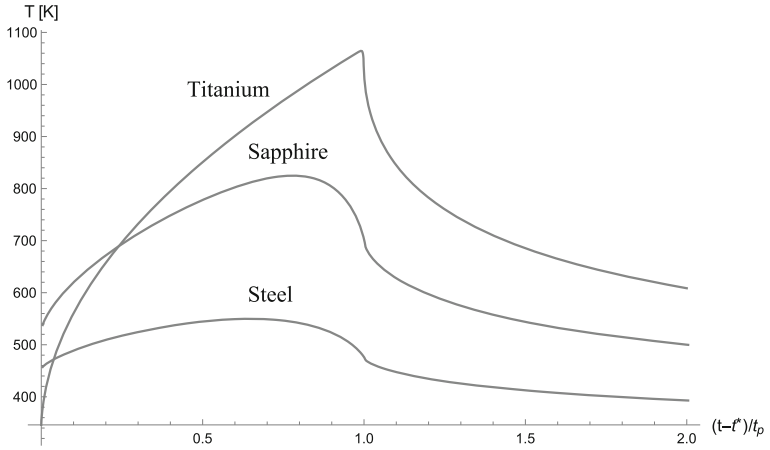

Fig. 6 Temperature evolution at the edge workpiece during the cut-out transient regime

Figure 7 shows the evolution of the absolute temperature at the workpiece edge for the three data sets during the cut-in transient regime, i.e. $T^{\text{in}}_{w/2}(t, 0, 0)$. Note that all the graphs depart from room temperature T_0, since that is the temperature of the workpiece at $t = 0$. Notice as well that the maximum temperature occurs at $t_{\max} = t_{\text{p}}$, according to Theorem 1.

5.2 FEM analysis

In order to solve the heat transfer boundary problem during the transient regime using a numerical approach, we have considered the Cartesian coordinate system fixed to the

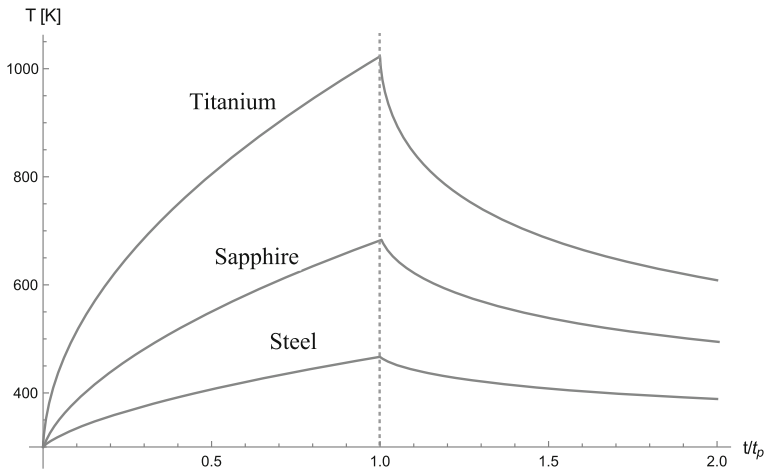

Fig. 7 Temperature evolution at the edge workpiece during the cut-in transient regime

workpiece (i.e. $X'Y'Z'$ in Figs. 3 and 4). Therefore, we have to solve the heat equation

$$\frac{\partial T}{\partial t} = \alpha \left(\frac{\partial^2 T}{\partial x'^2} + \frac{\partial^2 T}{\partial y'^2} \right), \tag{66}$$

subjected to the initial condition

$$T\left(0, x', y'\right) = T_0. \tag{67}$$

and a boundary condition given by

$$k \frac{\partial T}{\partial y}\left(t, x', 0\right) = d\left(t, x'\right), \tag{68}$$

where now the heat source is moving over the surface of the workpiece. The friction function $d\left(t, x'\right)$ for the cut-in and cut-out is,respectively,

$$d_{\text{in}}\left(t, x'\right) = -q\,\theta\left(x' - \max\left(v_{\text{d}} t - \delta, 0\right)\right)\theta\left(v_{\text{d}} t - x'\right),$$
$$d_{\text{out}}\left(t, x'\right) = -q\,\theta\left(x' - \min\left(v_{\text{d}}\left(t - t^*\right) - \delta, 0\right)\right)\theta\left(\min\left(v_{\text{d}}\left(t - t^*\right), 0\right) - x'\right).$$

In the analytic approach, we have considered that the workpiece is infinite (a quadrant in Cartesian coordinates). However, for the numerical solution of (66)–(68), we have to consider a finite region. According to Fig. 3, the length of the workpiece L has to be at least $\delta^* + \delta$, thus we have set

$$L = v_{\text{d}} t^* + \delta. \tag{69}$$

Also, it is known that the depth of thermal penetration δ_{p} is very shallow beneath the surface of the workpiece. In order to estimate δ_{p}, we have used the 1D approximation

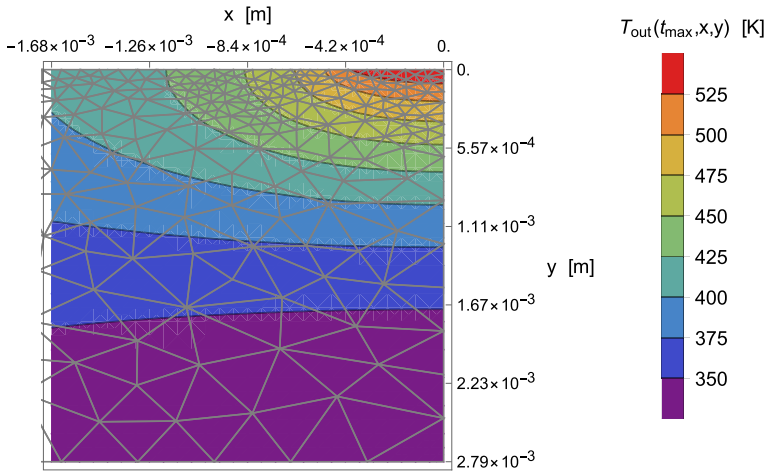

Fig. 8 FEM mesh and temperature field at $t = t_{\max}$ for the cut-out transient regime, considering data set 2

given in [28]:

$$\delta_{\mathrm{p}} = 2\sqrt{\alpha\, t_{\mathrm{p}}}\, g^{-1}(p)\,,$$

where

$$g(x) = \mathrm{e}^{-x^2} - \sqrt{\pi}\, x\, \mathrm{erfc}(x)\,,$$

and p is the fraction between the temperature rise at δ_{p} below the surface and the temperature rise on the surface. For the FEM analysis, we have set the workpiece depth H as

$$H = \delta_{0.01}.$$

Also, it is known that the temperature field gradient is very high nearby the contact zone between the grinding wheel and the surface [29]. Consequently, in order to obtain an accurate solution using FEM analysis, we need to use a mesh with more nodes where the gradient is higher. As an example of the latter, Fig. 8 shows the temperature field during the cut-out for data set 2 at $t = t_{\max}$ as well as the mesh used.

For the time interval used in the FEM analysis, we have used $t \in \left(0, 2\,t_{\mathrm{p}} + t^*\right)$ for the cut-out, and $t \in \left(0, 2\,t_{\mathrm{p}}\right)$ for the cut-in.

Finally, according to (69), note that we need to estimate the relaxation time t^* (hence the calculation of $X_{\max}$) in order to apply FEM analysis to the transient regime. Therefore, the analytic approach is essential to solve the transient regime, although we use a numerical approach.

Table 3 Maximum temperature $T_{\max}$ [K]

	Data 1	Data 2	Data 3
Cut-out			
FEM			
$T_{\max}^{\text{out, piece}}$	1064.43	546.95	815.49
Analysis			
$T_{\max}^{\text{out, edge}}$	1063.87	546.95	815.49
Analytic $T_{\max}^{\text{out}}$	1064.57	545.70	815.29
Cut-in			
FEM			
$T_{\max}^{\text{in, piece}}$	1043.97	482.29	717.26
Analysis			
$T_{\max}^{\text{in, edge}}$	1023.08	467.44	679.95
Analytic $T_{\max}^{\text{in}}$	1022.86	466.86	679.10
Stationary regime $T_{\max}^{\text{Sta}}$	1042.23	490.98	726.06

5.3 Analytic vs. numeric approach

Table 3 shows the maximum temperature $T_{\max}$ evaluated for the different regimes considered (i.e. stationary regime, and cut-out and cut-in transient regimes) by using both analytic and FEM approaches. For the FEM analysis, we have computed the maximum temperature at the edge both during cut-out and cut-in (i.e. $T_{\max}^{\text{out, edge}}$ and $T_{\max}^{\text{in, edge}}$), and at the whole workpiece (i.e. $T_{\max}^{\text{out, piece}}$ and $T_{\max}^{\text{in, piece}}$). For this purpose, we have applied NMaximize MATHEMATICA command, using the Differential Evolution method [30], which seems to be quite efficient in this case. Using this numerical method, it is worth noting that the location of the maximum temperature in the cut-out $(t_{\text{num}}, x_{\text{num}}, y_{\text{num}})$ is extremely near to the analytical approach, i.e. $(t_{\text{num}}, x_{\text{num}}, y_{\text{num}}) \approx (t_{\max}, 0, 0)$.

Within the analytic approach, the computation of the maximum temperature in the stationary regime $T_{\max}^{\text{Sta}}$ has been evaluated solving (16) with Newton's method, where we have taken $X = 0$ as starting iteration point. Once $X_{\max}$ is evaluated, we compute the maximum temperature in the stationary regime applying (17). For the computation of the maximum temperature during the cut-out $T_{\max}^{\text{out}}$, Brent's method [31] has been used for the root finding of $t_{\max}$ in (42) since the root interval is known. Once $t_{\max}$ is numerically evaluated, $T_{\max}^{\text{out}}$ is computed applying (36). Finally, the maximum temperature at the edge during the cut-in $T_{\max}^{\text{in}}$ is computed with (55).

Notice that $T_{\max}^{\text{out, edge}} \approx T_{\max}^{\text{out}}$ and $T_{\max}^{\text{in, edge}} \approx T_{\max}^{\text{in}}$ for all data sets, which validates the analytic model described above for the calculation of the maximum temperature at the edge during the transient regime. Moreover, $T_{\max}^{\text{out, piece}} \approx T_{\max}^{\text{out}}$ for all data sets, thus the analytic model also predicts the maximum temperature during the cut-out, which occurs at the final edge of the workpiece. Notice as well that $T_{\max}^{\text{out}} > T_{\max}^{\text{Sta}}$ for all data sets, so that the analytic model predicts a higher risk of thermal damage during the

Table 4 Computation times of the maximum temperature, t_{comp} [s]

	Data 1	Data 2	Data 3
Cut-out			
FEM	108.3	106.0	133.5
Analytic	0.248	0.127	0.131
Cut-in			
FEM	137.0	21.36	46.96
Analytic	0.022	0.013	0.014

cut-out, which agrees with [32]. However, notice that $T_{\max}^{\text{in}} < T_{\max}^{\text{in, piece}} \lesssim T_{\max}^{\text{Sta}}$ for all data sets. This means that the thermal damage risk during the cut-in transient regime is lower than in the stationary regime. Moreover, since the numerical time interval used in the FEM analysis for the cut-in is $t \in \left(0, 2\,t_{\text{p}}\right)$ and, according to Table 2, $2\,t_{\text{p}} > t^*$ for data set 1, we have $T_{\max}^{\text{in, piece}} \approx T_{\max}^{\text{Sta}}$ in this case. However, $2\,t_{\text{p}} < t^*$ for data sets 2 and 3, so that $T_{\max}^{\text{in, piece}} < T_{\max}^{\text{Sta}}$.

The great advantage of the analytical approach is its great speed in evaluating the maximum temperature in the transient regime. Table 4 shows the computation times t_{comp} of the maximum temperature $T_{\max}$ for both the analytical and numerical approaches. In the case of FEM analysis, t_{comp} is the sum of the computation time of the numerical evaluation of $T\,(t, x, y)$ and its maximum $T_{\max}$, as well as the computation time of t^* and $X_{\max}$. In the case of the analytical approach, t_{comp} is the sum of the computation time of $X_{\max}$, t^* and $T_{\max}$. It is apparent that the analytical approach is extremely faster than the numerical one ($\approx$ 1000 times faster). Note also that t_{comp} is much smaller for the cut-in than for the cut-out in the analytic approach because we have to numerically solve (42) in the former, but $t_{\max} = t_p$ in the latter, due to Theorem 1. Further, the numerical evaluation of t^* is very fast since the approximation given in (21) is quite good according to Table 2.

6 Conclusions

By using the $T^{(0)}$ Theorem [11] of the Samara–Valencia model [9], we have given analytical expressions for the evolution of the temperature field during the cut-in (48) and cut-out (32) transient regimes in surface grinding with adiabatic conditions (dry case), considering a constant heat flux profile within the contact zone between wheel and workpiece. For this purpose, we have used (22) in order to estimate the relaxation time of the stationary regime, turning out that is quite accurate for different grinding regimes (see Table 2). Also, we have numerically validated this analytic model for the transient regimes using FEM analysis. In this sense, we have obtained an excellent agreement for the maximum temperature during the cut-out. This is very useful for the prediction of thermal damage risk since the maximum temperature during the cut-out is higher than in the stationary regime. Further, the model predicts that this maximum is always located at the final edge of the workpiece. In addition, the model predicts that the maximum temperature at the initial edge during the cut-in is lower

than the maximum temperature in the stationary regime. These predictions agree with the experimental evidence [5].

The great advantage of the analytical approach described in this paper is that we can compute very rapidly the maximum temperature, both in the transient and in the stationary regimes. Further, theorem 1 allows to compute extremely rapid the maximum temperature at the initial edge during the cut-in. As aforementioned, all the analytical results presented in this paper are intended to offer a very useful analytical tool for monitoring online the grinding process in order to predict thermal damage risk during the transient regime. The graphs and results given in this paper have been performed with MATHEMATICA, and they are available at https://rb.gy/wffdne.

Author Contributions All the contents of the manuscript have been prepared, written and reviewed by the author.

Funding Open Access funding provided thanks to the CRUE-CSIC agreement with Springer Nature.

Declarations

Conflict of interest The author has no relevant financial or non-financial interests to disclose. The authors declare no competing interests.

Editorial Policies for Springer journals and proceedings https://www.springer.com/gp/editorial-policies. *Nature Portfolio journals* https://www.nature.com/nature-research/editorial-policies. *Scientific Reports* https://www.nature.com/srep/journal-policies/editorial-policies BMC journals: https://www.biomedcentral.com/getpublished/editorial-policies

Appendix A: The max and min functions

The max (x, y) and min (x, y) functions are defined as

$$\max(x, y) = \begin{cases} x, & x \geq y, \\ y, & x \leq y, \end{cases} \tag{A1}$$

and

$$\min(x, y) = \begin{cases} x, & x \leq y, \\ y, & x \geq y. \end{cases} \tag{A2}$$

According to [33, p. 16], these functions can be expressed as

$$\max(x, y) = \frac{x + y + |y - x|}{2}, \tag{A3}$$

$$\min(x, y) = \frac{x + y - |y - x|}{2}. \tag{A4}$$

From (A3) and (A4), it is very easy to prove that

$$f(x) - \max(f(x), 0) = \min(f(x), 0). \tag{A5}$$

Also, from (A2), we have

$$\frac{\mathrm{d}}{\mathrm{d}x} \min(f(x), a) = \begin{cases} f'(x), & f(x) > a, \\ & f(x) \neq a, \\ 0, & f(x) < a, \end{cases} \tag{A6}$$

that is

$$\frac{\mathrm{d}}{\mathrm{d}x} \min(f(x), a) = f'(x)\,\theta(f(x) - a), \quad f(x) \neq a. \tag{A7}$$

Theorem 2 *If $a, b \in \mathbb{R}$ and $a < b$, then*

$$\frac{\mathrm{d}}{\mathrm{d}x} \min(\max(f(x), a), b) = f'(x)\,\theta(f(x) - a)\,\theta(b - f(x)). \tag{A8}$$

Proof Consider the function

$$F(x) = \min(\max(f(x), a), b), \quad a < b. \tag{A9}$$

According to (A2), we have

$$F(x) = \begin{cases} \max(f(x), a), & \max(f(x), a) \leq b, \\ & \\ b, & \max(f(x), a) \geq b. \end{cases} \tag{A10}$$

Since $a < b$, then the condition $\max(f(x), a) \leq b$ (or $\max(f(x), a) \geq b$) is equivalent to $f(x) \leq b$ (or $f(x) \geq b$), thus, applying now (A1) to (A10) we have

$$F(x) = \begin{cases} f(x), & a \leq f(x) \leq b, \\ & \\ a, & f(x) \leq a, \\ & \\ b, & f(x) \geq b. \end{cases} \tag{A11}$$

Performing the derivative in (A11)

$$F'(x) = \begin{cases} f'(x), & a \leq f(x) \leq b, \\ 0, & f(x) \leq a, \qquad f(x) \neq a, b, \\ 0, & f(x) \geq b, \end{cases} \tag{A12}$$

thus

$$F'(x) = f'(x)\,\theta(f(x)-a)\,\theta(b-f(x)), \quad f(x) \neq a, b. \tag{A13}$$

□

Theorem 3 *If $a, b \in \mathbb{R}$ and $a < b$, then*

$$1-\theta(f(x)-a)\,\theta(b-f(x)) = \theta(a-f(x)) + \theta(f(x)-b). \tag{A14}$$

Proof According to [21, Eq. 9:5:1], we have

$$\theta(a-f(x)) = 1-\theta(f(x)-a). \tag{A15}$$

Thereby,

$$\begin{aligned} 1-\theta(f(x)-a)\,\theta(b-f(x)) &= 1-[1-\theta(a-f(x))][1-\theta(f(x)-b)] \\ &= \theta(a-f(x)) + \theta(f(x)-b), \end{aligned}$$

since

$$\theta(a-f(x))\,\theta(f(x)-b) = 0, \tag{A16}$$

for $a < b$. □

Theorem 4 *If $f(x)$ is a real function and $a, b \in \mathbb{R}$ with $a < b$, then*

$$\begin{aligned} &\min(\max(f(x), a), b) - f(x) \\ &= \theta(a-f(x))[a-f(x)] + \theta(f(x)-b)[b-f(x)]. \end{aligned} \tag{A17}$$

Proof Indeed, according to (A9) and (A11), we have

$$\begin{aligned} F(x) - f(x) &= \min(\max(f(x), a), b) - f(x) \\ &= \begin{cases} 0, & a \leq f(x) \leq b, \\ a-f(x), & f(x) \leq a, \\ b-f(x), & f(x) \geq b. \end{cases} \end{aligned} \tag{A18}$$

Therefore, we can rewrite (A17) as (A18). □

References

1. Malkin S, Guo C (2008) Grinding Technology: Theory and Application of Machining with Abrasives. Industrial Press, New York
2. Outwater JO, Shaw MC (1952) Surface temperatures in grinding. J Eng Ind Trans ASME 74(1):73–81
3. Hegeman JBJW, De Hosson JTM, De With G (2001) Grinding of WC-Co hardmetals. Wear 248(1–2):187–196
4. González-Santander JL (2014) Calculation of an integral arising in dry flat grinding for a general heat flux profile. Application to maximum temperature evaluation. J Eng Math 88(1):137–160
5. Guo C, Malkin S (1995) Analysis of transient temperatures in grinding. J Manuf Sci E Trans ASME 57:571–577
6. Jaeger JC (1942) Moving sources of heat and the temperature at sliding contacts. Proc R Soc New South Wales 76:204–224
7. Rowe WB, Jin T (2001) Temperatures in high efficiency deep grinding (HEDG). CIRP Ann 50(1):205–208
8. Carslaw HS, Jaeger JC (1986) Conduction of heat in solids. Oxford Science Publications, Oxford
9. Skuratov DL, Ratis YL, Selezneva IA, Pérez J, Córdoba P, Urchueguía JF (2007) Mathematical modelling and analytical solution for workpiece temperature in grinding. Appl Math Model 31(6):1039–1047
10. Ju Y, Farris TN, Chandrasekar S (1998) Theoretical analysis of heat partition and temperatures in grinding. J Tribol Trans ASME 120:789–794
11. González-Santander JL, Valdés Placeres JM, Isidro JM (2011) Exact solution for the time-dependent temperature field in dry grinding: application to segmental wheels. Math Probl Eng 2011: Article ID 927876
12. Jin T, Stephenson DJ (2004) Three dimensional finite element simulation of transient heat transfer in high efficiency deep grinding. CIRP Ann 53(1):259–262
13. González-Santander JL (2016) Analytic solution for maximum temperature during cut in and cut out in surface dry grinding. Appl Math Model 40(3):2356–2367
14. Shaw MC (1990) Temperatures in cutting and grinding. ASME 146:17–24
15. Lavine AS, Malkin S, Jen TC (1989) Thermal aspects of grinding with CBN wheels. CIRP Ann 38(1):557–560
16. Guo C, Malkin S (1995) Analysis of energy partition in grinding. J Eng Ind 117:55–61
17. Zhang LC, Suto T, Noguchi TH, Waida T (1992) An overview of applied mechanics in grinding. Manuf Rev 5(4):261–273
18. Rowe WB, Black SCE, Mills B, Qi HS, Morgan MN (1995) Experimental investigation of heat transfer in grinding. CIRP Ann 44(1):329–332
19. Olver FWJ, Lozier DW, Boisvert RF, Clark CW (2010) NIST handbook of mathematical functions. Cambridge University Press, Cambrigde
20. González-Santander JL, Monreal L (2019) Efficient temperature field evaluation in wet surface grinding for arbitrary heat flux profile. J Eng Math 116:101–122
21. Oldham KB, Myland J, Spanier J (2009) An atlas of functions: with equator, the atlas function calculator, 2nd edn. Springer, New York
22. González-Santander JL, Martín G (2015) A theorem for finding maximum temperature in wet grinding. Math Probl Eng 2015:1–13
23. González-Santander JL (2017) Efficient series expansions of the temperature field in dry surface grinding for usual heat flux profiles. Math Probl Eng 2017: Article ID 1856523
24. Corless RM, Gonnet GH, Hare DEG, Jeffrey DJ, Knuth DE (1996) On the Lambert W function. Adv Comput Math 5(1):329–359
25. Haberman R (1987) Elementary applied partial differential equations: with fourier series and boundary value problems. Prentice Hall, Hoboken
26. Murav'ev VI, Yakimov AV, Chernyshev AV (2003) Effect of deformation, welding, and electrocontact heating on the properties of titanium alloy VT20 in pressed and welded structures. Met Sci Heat Treat 45(11–12):419–422
27. Lavine AS (1988) A simple model for convective cooling during the grinding process. J Eng Ind 110:1–6
28. González-Santander JL, Espinós-Morató H (2018) Depth of thermal penetration in straight grinding. Int J Adv Manuf Technol 96:3175–3190

29. Anderson D, Warkentin A, Bauer R (2008) Experimental validation of numerical thermal models for dry grinding. J Mater Process Technol 204(1–3):269–278
30. Georgioudakis M, Plevris V (2020) A comparative study of differential evolution variants in constrained structural optimization. Front Built Environ 6:102
31. Brent RP (1973) Algorithms for minimization without derivatives. Prentice Hall, Englewood Cliffs
32. Guo C (1993) Investigation of Fluid Flow and Heat Transfer in Grinding. PhD thesis, University of Massachusetts
33. Spivak M (2006) Calculus, 3rd edn. Cambridge University Press, Cambridge